PAPER

Polyacrylonitrile/polyaniline core/shell nanofiber mat for removal of hexavalent chromium from aqueous solution: mechanism and applications†

Jianqiang Wang,[a] Kai Pan,*[ab] Emmanuel P. Giannelis[bc] and Bing Cao*[a]

Polyacrylonitrile/polyaniline core/shell nanofibers were prepared *via* electrospinning followed by *in situ* polymerization of aniline. Nanofibers with different morphology were obtained by changing the polymerization temperature. When used as absorbent for Cr(VI) ions, the core/shell nanofiber mats exhibit excellent adsorption capability. The equilibrium capacity is 24.96, 37.24, and 52.00 mg g^{-1} for 105, 156, and 207 mg L^{-1} initial Cr(VI) solution, respectively, and the adsorption capacity increases with temperature. The adsorption follows a pseudo second order kinetics model and is best fit using the Langmuir isotherm model. The mats show excellent selectivity towards Cr(VI) ions in the presence of competing ions albeit a small decrease in adsorption is observed. The mats can be regenerated and reused after treatment with NaOH making them promising candidates as practical adsorbents for Cr(VI) removal.

Introduction

Recently, water safety has attracted more and more attention, especially heavy metal ions pollution. One of the most toxic pollutants is hexavalent chromium, which is generated by electroplating, metal finishing, leather tanning, photography, dye and textiles industries. Chromium exists in the environment in both trivalent (Cr(III)) and hexavalent (Cr(VI)) forms. Trivalent chromium is considered as an essential micronutrient for human, plant and animal metabolism. Cr(VI) is more toxic than Cr(III), and carcinogenic to living organisms.[1] The World Health Organization (WHO) recommends the maximum allowable limit for discharge of Cr(VI) into drinking water is 0.05 mg L^{-1}. Therefore, it is necessary to develop simple and effective methods to remove Cr(VI) from aqueous solution streams, in order to avoid deleterious impact of Cr(VI) on human health.

In general, electrochemical reduction,[2] electrocoagulation,[3] ion exchange,[4–7] membrane separation,[8–10] and adsorption[11–20] have been used for the removal of heavy metal ions. Among these methods, adsorption is simple and effective. Different

kinds of materials have been used as adsorbents for heavy metal ions, such as active carbon, metal oxide nanoparticles, mesoporous materials and agriculture waste, *etc.* Although these materials show good performance for removal of Cr(VI) from aqueous solutions, an additional separation step to remove the adsorbents out of the solution is required. To circumvent this problem, some have used a polymer fiber mat as adsorbent. For example, polyacrylonitrile (PAN) fibers with amine groups were used for the removal of Cu^{2+} and CrO$_4$$^{2-}$.[21,22] Recently polymer nanofiber mats obtained by electrospinning were used as base material for the adsorbent because of their small diameter and ease of preparation. These kinds of adsorbents not only have large surface area and adjustable surface functional groups, but also eliminate the separation step. Chitosan and aminated electrospun PAN nanofiber mats were used for the removal of Cu^{2+}, Ag$^+$ and Pb^{2+}.[23–25] Hydrolysis was used for the modification of ultrafine PAN nanofiber mats and its adsorption performance for Cu^{2+} was studied.[26] Polyethyleneimine nanofiber mat, with a large amount of amino and imino groups in its polymer chain, was also obtained by direct electrospinning directly and used for adsorption of Cu^{2+}, Pb^{2+} and Cd^{2+}.[27,28] The main focus of all these systems has been the removal of Cu^{2+} and Pb^{2+} by using amine or imine groups. Since Cr(VI) ion is toxic for human health, it is necessary to develop effective materials and simple methods for its removal from aqueous solutions. PAN/ferrous chloride (FeCl$_2$) composite porous nanofibers and PAN@γ-AlOOH fiber films based on electrospinning technology have already been used for Cr removal from aqueous solution.[29,30] Motivated by the work of core–shell materials[31] and polypyrrole functionalized materials,[32–34] a PAN/PPy core/

[a]Key Laboratory of Carbon Fiber and Functional Polymers (Ministry of Education), Beijing University of Chemical Technology, Beijing, P. R. China. E-mail: pankai@mail.buct.edu.cn; bcao@mail.buct.edu.cn; Fax: 86-10 6443 6876; Tel: 86-10 6441 3857

[b]Department of Materials Science and Engineering, Cornell University, Ithaca, NY, USA

[c]Center for Refining & Petrochemicals, KFUPM, Dhahran, 31261, Saudi Arabia
† Electronic supplementary information (ESI) available: Diameter distribution of PAN and PAN/PANI nanofibers, adsorption capacity of PAN/PANI nanofiber mat prepared at different temperatures, and morphology of PAN/PANI nanofiber mat after regenerated by NaOH for 5 times. See DOI: 10.1039/c3ra40616d

shell nanofiber mat was prepared and used for the Cr(VI) removal.[35] As previously reported in the literatures,[36–38] polyaniline (another typical conductive polymer) shows excellent Cr removal performance from aqueous solution. Polyaniline doped with sulfuric acid, polyaniline nanowire and polyaniline coated Kapok fiber were used for the removal of Cr(VI) from aqueous solution.

Inspired by the work above, we have chosen PAN nanofiber mats (obtained by electrospinning) as a template to obtain polyacrylonitrile/polyaniline core/shell structure nanofiber. The Cr(VI) removal performance was studied with an emphasis on understanding the adsorption mechanism in order to better understand the adsorption process.

Experimental

Chemicals

Polyacylonitrile (PAN, Mn 150 000) was purchased from Sigma-Aldrich. Potassium dichromate ($K_2Cr_2O_7$), dimethylformamide (DMF) and sulfuric acid are analytical reagent grade from Beijing Chemical Co., Ltd. Ammonium persulfate ((NH_4)$_2S_2O_8$) is analytical reagent grade from Xilong Chemical Co., Ltd. Aniline (99.5%) was purchased from Tianjin Guangfu Technology Development Co., Ltd and used after distillation.

Apparatus and instrumentation

The functional groups on the surface of the synthesized adsorbents were detected by attenuated total reflections Fourier transform infrared (ATR-FTIR) spectrometer using a Perkin-Elmer Spectrum RX I with a resolution of 4 cm^{-1}. Surface chemical compositions of pristine PAN nanofibers and functionalized nanofibers were analyzed by X-ray photoelectron spectroscopy (XPS) using Thermo Electron Corporation ESCALAB250 equipment with an Al Kα X-ray source (1486.6 eV). Surface morphology and structures of the nanofiber mat were studied using a Hitachi S-4700 scanning electron microscopy (SEM) and a Hitachi-800 transmission electron microscope (TEM). Cr(VI) concentration was measured by an inductively coupled plasma mass spectrometry (7700 series, Agilent technologies).

Electrospinning of PAN nanofiber mat

The procedure for electrospinning of PAN nanofiber mat was as follows. PAN was dissolved in DMF and stirred at 60 °C for 12 h to obtain 8 wt% homogeneous solutions. PAN nanofibers were collected on the aluminum foil at a high voltage of 14 kV. The solution feed rate was 1.2 mL h^{-1} and the spinneret diameter was 0.7 mm. The distance between collector and spinneret was 10 cm. A rotating metal drum (diameter: 10 cm, length: 26 cm, rotating speed: 80 rpm) was used to collect the deposited nanofibers during the electrospinning process. To obtain a uniform electrospinning nanofiber mat with sufficient area, a stepping motor was used to control the translational oscillatory motion perpendicular to the drum rotation direction (the oscillation distance was about 25 cm). The thickness of the nanofiber mat is about 50 μm.

Scheme 1 Schematic illustration of PAN/PANI nanofiber preparation.

Preparation of PAN/PANI core/shell nanofiber mat

The PAN/PANI core/shell nanofiber mat was synthesized *via in situ* chemical oxidative polymerization technique. A typical preparation process is shown schematically in Scheme 1. In a typical procedure, 1.0 g (NH_4)$_2S_2O_8$ and 1.0 g aniline were dissolved in 8 mL and 33 mL 1 M HCl respectively. Four pieces (about 4 cm × 4 cm) of PAN nanofiber mat were added into the aniline HCl solution and the (NH_4)$_2S_2O_8$ was added into the beaker to start the polymerization. Three different temperatures (0 °C, 16 °C and 35 °C) were studied. The mixture was shaken at 100 rpm in a thermostatic shaker bath operating at the desired temperature. The PAN nanofiber mat was taken out 2 h later, washed with deionized water repeatedly to remove the residual aniline monomers, and then dried in vacuum overnight.

Cr(VI) adsorption experiments

$K_2Cr_2O_7$ was used as the source of Cr(VI). 100 mg dry PAN/PANI nanofiber mats were directly added into a beaker containing 30 mL 200 ppm Cr(VI) solutions at different pHs for 12 h. During this process, the beaker was shaken in a thermostatic shaker bath, operating at 25 °C and 100 rpm. The pH of the Cr(VI) solution was adjusted by adding 0.5 M HCl. The removal percentage of Cr(VI) was calculated using the following equation:

$$\% \text{ removal} = \frac{C_0 - C_e}{C_0} \qquad (1)$$

where C_0 is the initial concentration of Cr(VI) in solution (mg L^{-1}) and C_e is the equilibrium concentration (mg L^{-1}).

The adsorption isotherms for Cr(VI) were established by batch adsorption experiments. 100 mg PAN/PANI nanofiber mat was immersed into 30 mL Cr(VI) solutions with different concentration. The initial pH of Cr(VI) solutions was adjusted to 2.0 by using 0.5 M HCl. The adsorption was carried out at 25 °C with constant shaking, and then kept for 12 h to establish adsorption equilibrium. The equilibrium adsorption capacity was determined using the following equation:

$$q_e = \frac{C_0 - C_e}{m} V \qquad (2)$$

where C_0 is the initial concentration of Cr(VI) in solution (mg L^{-1}), C_e is the equilibrium concentration (mg L^{-1}), q_e is the

equilibrium adsorption capacity (mg L^{-1}), m is the mass of adsorbent (g), and V is the volume of solution (L), respectively.

The kinetic adsorption performance was studied by contacting 100 mg of PAN/PANI nanofiber mat with Cr(VI) solutions of different initial concentration at 25 °C. The initial pH of Cr(VI) solution is 2.0, and the solution was shaken in a thermostatic shaker bath during the process. 0.05 mL aliquots were taken at different time and tested. The adsorption capacity was calculated by the following equation:

$$q_t = \frac{C_0 - C_t}{m} V \qquad (3)$$

where q_t is the adsorption capacity at time t, C_0 is the initial concentration of Cr(VI) in solution (mg L^{-1}), C_t is the Cr(VI) concentration at time t (mg L^{-1}), m is the mass of adsorbent (g), and V is the volume of solution (L), respectively.

Desorption experiments

For desorption studies, 100 mg PAN/PANI nanofiber mat was first contacted with 30 mL 180 mg L^{-1} Cr(VI) for 12 h at 25 °C. Then the mats were immersed into 30 mL 0.002 M NaOH, 0.01 M NaOH or 0.05 M NaOH for 30 min at 25 °C, respectively. The above procedure was repeated 5 times to test the reusability of the adsorbents.

Results and discussion

ATR-FTIR study of PAN/PANI nanofibers

ATR-FTIR was used to study the surface compositions of PAN/PANI nanofibers, and the results are shown in Fig. 1. The absorption bands assigned to C=C stretching in quinoid and benzenoid segments appeared at 1495 cm^{-1} and 1580 cm^{-1}, respectively.[39] Besides the above, peaks at 1141 cm^{-1} and 1303 cm^{-1} are attributed to C–H bending and C–N stretching,

respectively.[39] These results confirm the presence of PANI coated on the surface of PAN nanofibers.

XPS analysis of PAN/PANI nanofiber mat

XPS was used to further study surface compositions of the nanofibers. The wide scan and N 1s peaks for pure PAN and PAN/PANI nanofiber mat are shown in Fig. 2. For pure PAN (Fig. 2b), the N 1s signal has one single component centred at about 398.1 eV due to C≡N groups from PAN chains. The N 1s core-level spectrum of PAN/PANI nanofiber mat prepared at 0 °C, 16 °C and 35 °C (Fig. 2d, 2f and 2h) can be fitted into four peak components with BEs of about 398.5, 399.6, 401.1, and 402.6 eV attributable to the =N–, –NH–, and N$^+$ species, respectively.[40] It was also observed that secondary amines (–NH–) were the main species present at all experimental conditions. All the above results indicate that uniform PANI layers were successfully coated on the surface of PAN nanofibers.
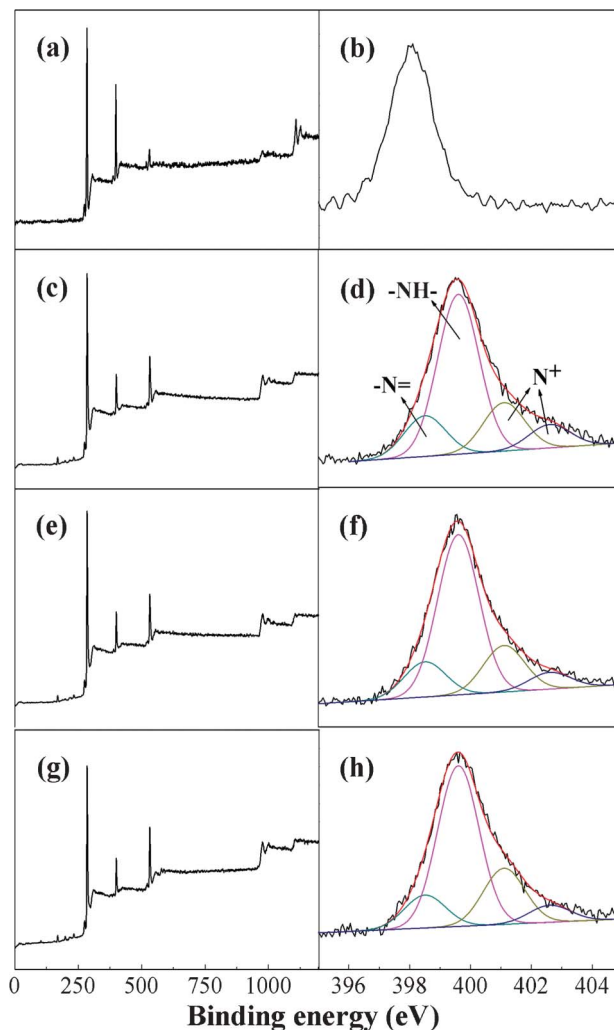

Fig. 1 ATR-FTIR spectra of pure PAN nanofiber mat (a), and PAN/PANI nanofiber mat prepared at different polymerization temperatures: 0 °C (b), 16 °C (c), 35 °C (d).

Fig. 2 XPS wide scan and N 1s core level spectra of pure PAN nanofibers (a and b), and PAN/PANI nanofibers prepared at different polymerization temperatures: 0 °C (c and d), 16 °C (e and f), 35 °C (g and h).
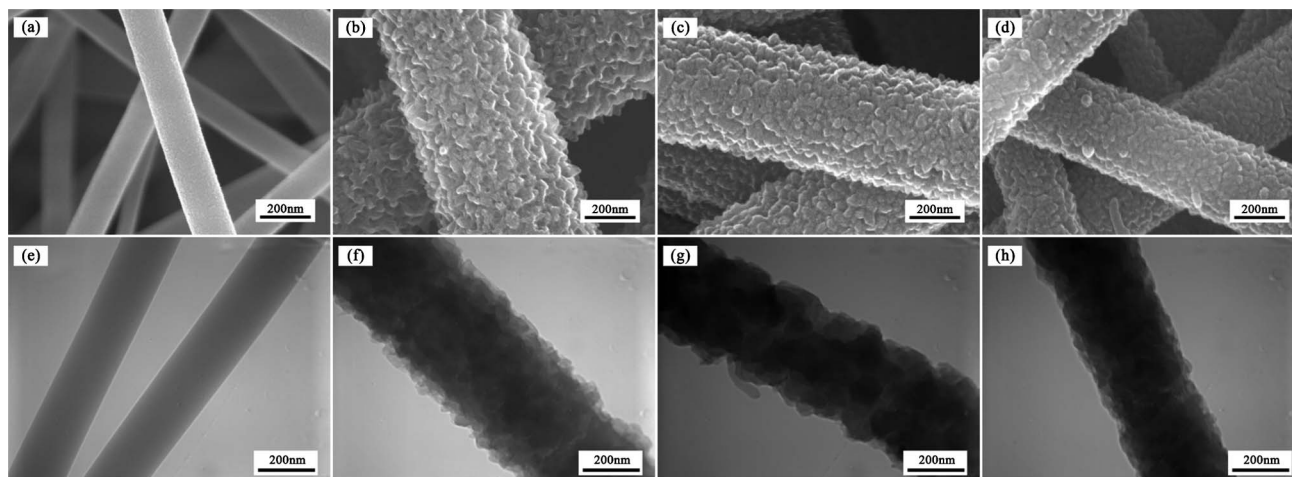
Fig. 3 SEM and TEM images of pure PAN nanofibers (a and e), and PAN/PANI nanofibers prepared at different polymerization temperatures: 0 °C (b and f), 16 °C (e and g), 35 °C (d and h).

Morphology of the nanofibers

The optical image of nanofiber mat can be obtained in Fig. S1, ESI.† The morphology of pure PAN and PAN/PANI nanofibers was studied by SEM and TEM, and the results are shown in Fig. 3. The core/shell structure can be clearly seen from TEM images as shown in Fig. 3f–3h. It was also observed that the surface of pure PAN nanofibers was smooth with an average diameter of about 200 nm (Fig. S2a, ESI†). After aniline polymerization on the surface of PAN nanofibers, the surface of PAN/PANI nanofibers became coarser, and the average diameter increased (Fig. S2b–S2d, ESI†). Meanwhile the porosity of the nanofiber mat decreased from 80% to 70% due to the increase of the nanofiber diameter (Table S1, ESI†). The roughness increased as the reaction temperature decreased. The increase of roughness might be beneficial as it increases the surface area and the number of available binding sites for adsorption. However, the adsorption capacity of PAN/PANI nanofiber mats prepared at different temperature is similar as shown in Fig. S3, ESI,†which may be due to the fiber diameter increase at low temperature.

pH effect on the adsorption

The initial solution pH has a great effect on the Cr(VI) adsorption. As reported in the literature,[41] the predominant Cr(VI) species are monovalent bichromate ($HCrO_4^-$) and divalent dichromate ($Cr_2O_7^{2-}$) ions when the pH is in the range of 2.0–6.0. As shown in Fig. 4, when the pH of the initial solution changed from 6.0 to 2.0, the adsorption capacity increased from 35.2 mg g^{-1} to 53.4 mg g^{-1} consistent with results previously reported in the literature.[33] The decrease of adsorption capacity as the pH increases is due to the competition between hydroxyl (OH^-) ions and CrO_4^{2-} ions for the same sorption sites on the sorbent surface. Based on the results, all subsequent adsorption isotherms and kinetic experiments were performed at initial pH of 2.0.

Effect of ionic strength

The effect of ionic strength on adsorption was studied by carrying out a series of experiments with solutions containing varying concentrations of NaCl. The pH of the Cr(VI) solutions with NaCl was adjusted to 2.0 before adsorption. The results are shown in Fig. 5. The adsorption capacity slightly decreased with an increase of ionic strength. The adsorption capacity still remains 90.4% of that without NaCl when the NaCl concentration increased to 0.1 mol L^{-1}. Therefore, the presence of Na^+ or Cl^- ions has a minimal effect on the adsorption process.

Adsorption kinetics

The effect of adsorption time on the adsorption capacity at different initial solution concentration is shown in Fig. 6. The results indicate that the adsorption capacity of Cr(VI) increases
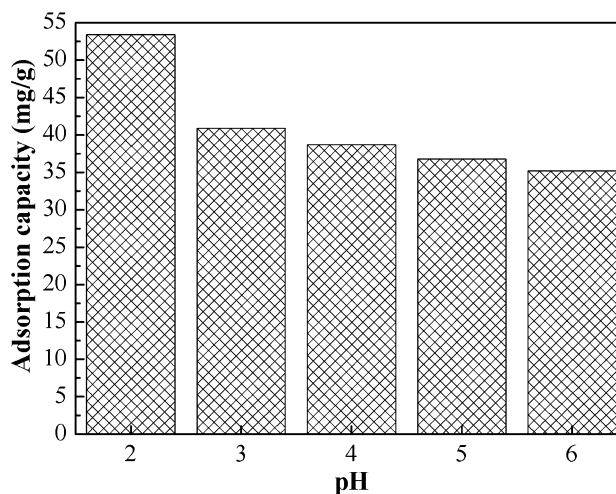

Fig. 4 Effect of pH on the adsorption capacity of Cr(VI) on PAN/PANI nanofiber mat.
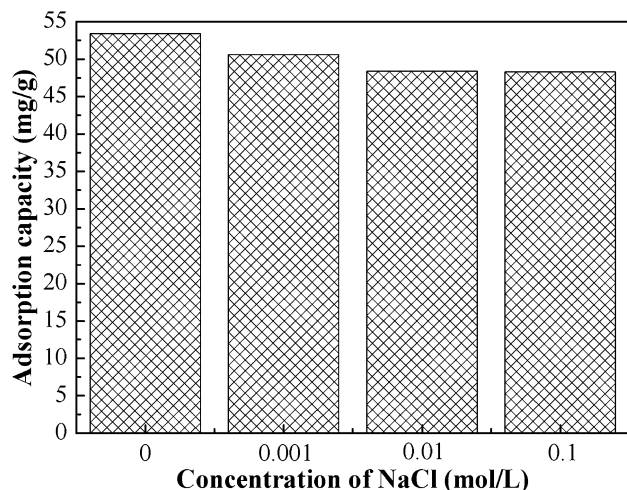
Fig. 5 Effect of ionic strength on the adsorption capacity of PAN/PANI nanofiber mat for Cr(VI).

with an increase of adsorption time until equilibrium is reached. The adsorption equilibrium was reached within 30 min as the initial solution concentration ranged from 105 to 207 mg L^{-1}. The equilibrium capacity is 24.96, 37.24, and 52.00 mg g^{-1} for 105, 156, and 207 mg L^{-1} initial Cr(VI) solution, respectively.

In order to better understand the adsorption behaviours, the adsorption kinetic data are often analyzed using two commonly used kinetic models,[42] namely, the pseudo-first-order, and the pseudo-second-order. These two kinetic models are used to describe the adsorption of solid/liquid systems, which can be expressed in the linear forms as eqn (4) and (5), respectively:

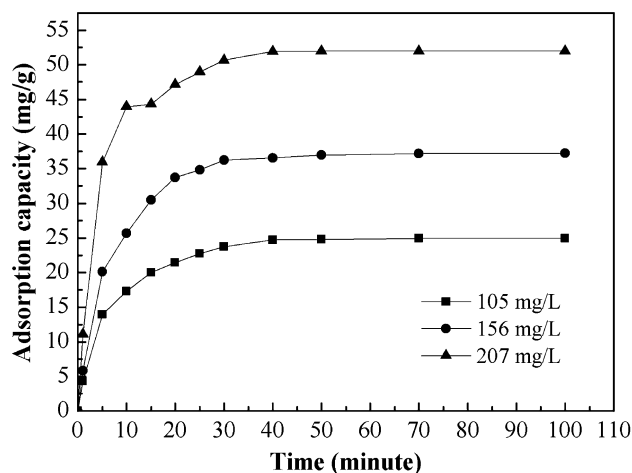$$\log(q_e - q_t) = \log q_e - \frac{K_1}{2.303}t \tag{4}$$

Fig. 6 Effect of contact time and initial concentration on the adsorption of Cr(VI) of PAN/PANI nanofiber mat.
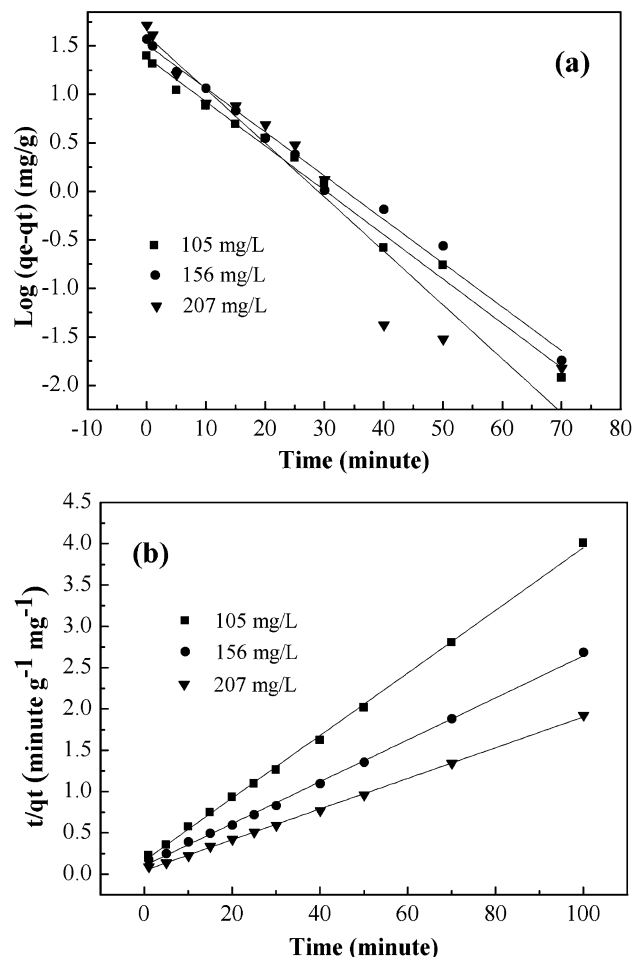

Fig. 7 Pseudo-first-order kinetic model (a), pseudo-second-order kinetic model (b) for adsorption of Cr(VI) onto PAN/PANI nanofiber mat.

$$\frac{t}{q_t} = \frac{1}{K_2 q_e^2} + \frac{1}{q_e}t \tag{5}$$

where K_1 and K_2 are the pseudo first order and second order rate constants, respectively.

The adsorption kinetic plots are shown in Fig. 7 and the obtained kinetic parameters are summarized in Table 1. The values of the correlation coefficients clearly indicated that the adsorption kinetics closely followed the pseudo-second-order model. The $q_{e,cal}$ values obtained from pseudo-second-order kinetic model appeared to be very close to the experimentally observed values.

Adsorption isotherm and thermodynamic study

Adsorption isotherms experiments were conducted to study the adsorption capacity of PAN/PANI nanofiber mat for Cr(VI) removal. The adsorption isotherms at 25 °C, 35 °C and 45 °C are shown in Fig. 8. The results indicate that there is an increase of adsorption capacity with an increase of solution temperature. The increase of adsorption capacity with the increase of initial concentration is faster at higher solution temperatures. This may be due to an increase in thermal

Table 1 Kinetics parameters for Cr(VI) adsorption onto PAN/PANI nanofiber mat

C_0 (mg L^{-1})	[a] $q_{e,exp}$ (mg g^{-1})	Pseudo-first-order model			Pseudo-second-order model		
		K_1 (min^{-1})	[b] $q_{e,cal}$ (mg g^{-1})	R^2	K_2 (g mg^{-1} min^{-1})	[b] $q_{e,cal}$ (mg g^{-1})	R^2
105	24.96	0.105	24.16	0.99030	8.78×10^{-3}	26.39	0.99805
156	37.24	0.104	32.55	0.99037	6.11×10^{-3}	39.38	0.99843
207	51.99	0.128	40.48	0.92303	7.20×10^{-3}	53.85	0.99933

[a] $q_{e,exp}$: equilibrium adsorption capacity from experiments. [b] $q_{e,cal}$: equilibrium adsorption capacity calculated from kinetic models.
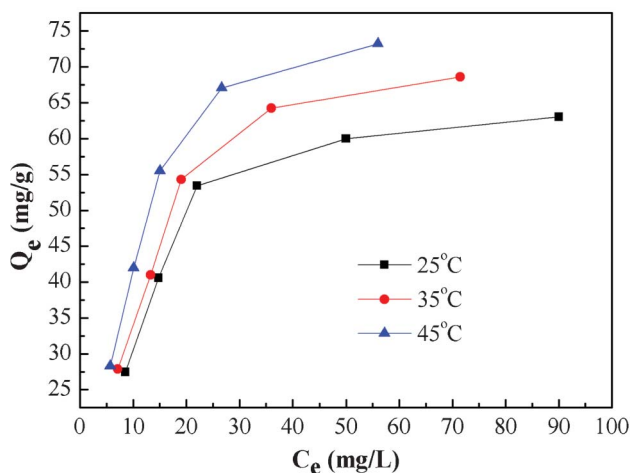
energy of the adsorbing species, which leads to higher adsorption capacity and faster adsorption rate. These results indicate that Cr(VI) adsorption by the PAN/PANI nanofiber mat is endothermic in nature. Two well-known models[43] (Langmuir and Freundlich) were used to fit the equilibrium data, and the correlation coefficient (R^2) obtained was used to evaluate the fit of the two models. The Langmuir model is based on assuming adsorption homogeneity, corresponding to equally available adsorption sites, monolayer surface coverage, and no interaction between adsorbed species. The linearized Langmuir isotherm model is represented by the following equation:

$$\frac{C_e}{q_e} = \frac{1}{q_m b} + \frac{C_e}{q_m} \qquad (6)$$

The Freundlich isotherm describes reversible adsorption and is not restricted to the formation of a monolayer. This empirical equation takes the form of eqn (7):

$$\ln q_e = \ln K_f + \frac{\ln C_e}{n} \qquad (7)$$

where q_m (mg g^{-1}) is the maximum adsorption capacity, b (L mg^{-1}) is the Langmuir constant related to the energy of adsorption, K_f and $1/n$ are constants related to the adsorption capacity and strength of adsorption, respectively.

The values of these parameters obtained from the plots in Fig. 9, are summarized in Table 2. The higher values of correlation coefficient reveal that the Langmuir model better fit the isotherm data. The maximum adsorption capacity calculated from the Langmuir model increases from 71.28 to 88.11 mg g^{-1} as the temperature increased from 25 to 45 °C.

The thermodynamic parameters associated with the adsorption process, standard Gibbs free energy change (ΔG^0), enthalpy change (ΔH^0), and entropy change (ΔS^0) were calculated using the following equations:[28,44]

Fig. 8 Equilibrium isotherms of Cr(VI) adsorption onto PAN/PANI nanofiber mat at different temperature.
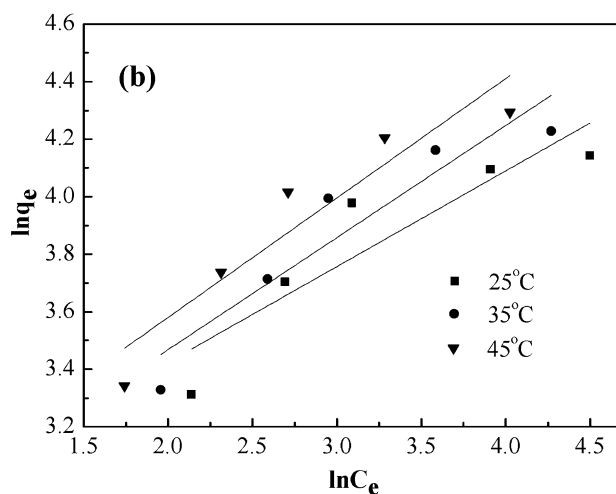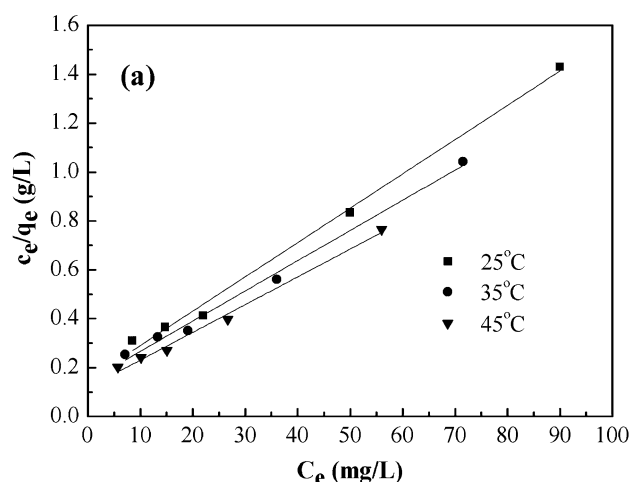

Fig. 9 Langmuir isotherm model (a), Freundlich isotherm model (b) for adsorption of Cr(VI) onto PAN/PANI nanofiber mat.

Table 2 Langmuir and Freundlich isotherm parameters

	Langmuir model			Freundlich model		
T/°C	q_m (mg g^{-1})	b (L mg^{-1})	R^2	K_f (mg g^{-1})	$1/n$	R^2
25	71.28	0.094	0.99335	15.65	0.33	0.78118
35	80.91	0.086	0.99164	14.72	0.39	0.84995
45	88.11	0.097	0.99130	15.77	0.42	0.86080

Table 3 Thermodynamic parameters for Cr(VI) uptake by PAN/PANI nanofiber mat

T/°C	ΔG^0 (kJ mol^{-1})	ΔH^0 (kJ mol^{-1})	ΔS^0 (J mol^{-1} K^{-1})
25	−2.91	69.63	259.67
35	−3.52		
45	−4.24		

$$\ln K_d = \frac{\Delta S^0}{R} + \frac{-\Delta H^0}{RT} \tag{8}$$

$$K_d = \frac{(C_0 - C_e)V}{mC_e} \tag{9}$$
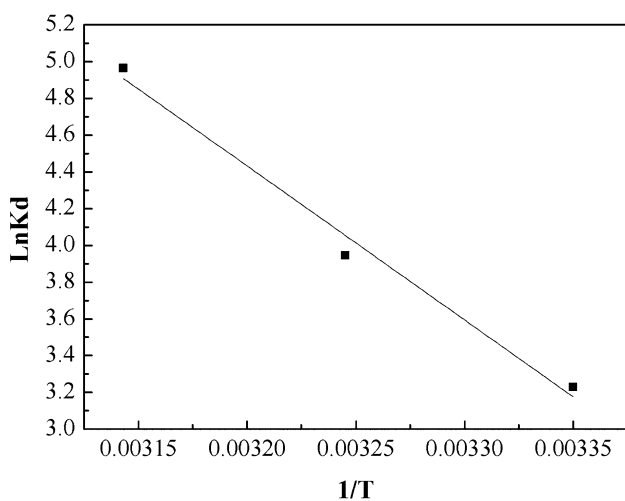
$$\Delta G^0 = -RT \ln K_d \tag{10}$$

where m is the adsorbent dose (g), R (J mol^{-1} K^{-1}) is the gas constant and T/K is the absolute solution temperature, respectively.

The values of ΔH^0 and ΔS^0 were obtained from the slope and intercept of the plot of $\ln K_d$ versus $1/T$ (shown in Fig. 10). The values of ΔG^0, ΔH^0 and ΔS^0 are presented in Table 3. From the plot, both the change in entropy (ΔS^0) and the enthalpy (ΔH^0) of adsorption were determined and are 259.67 J mol^{-1} K^{-1} and 69.63 kJ mol^{-1}, respectively. The positive value of ΔH^0 confirms that the adsorption process is endothermic. The positive entropy change (ΔS^0) indicates an increase in randomness at the PAN/PANI nanofibers-solution interface.

Competitive metal adsorption

In most cases, water contaminated with heavy metal ions contains several ionic species. Therefore, it is necessary to study the adsorp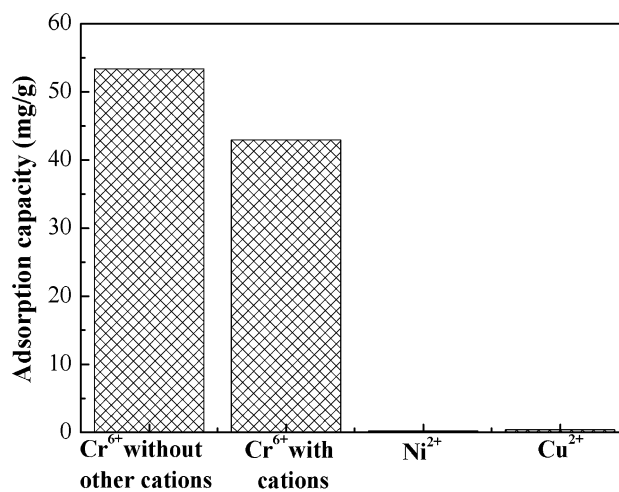tion performance in a mixed solution. In this study, we used Ni(II) and Cu(II) as the coexisting metal ions. About 100 mg PAN/PANI nanofiber mats were immersed into 30 mL mixed solution, which contains Cr(VI), Ni(II), and Cu(II). The initial concentration of each metal ion was 200 mg L^{-1}, and the solution pH was 2.0. Fig. 11 shows the effects of coexisting metal ions on Cr(VI) adsorption. The results indicated that Cr(VI) adsorption was slightly decreased due to the presence of Ni(II), and Cu(II) ions in solution. Importantly, the PAN/PANI nanofiber mat shows higher selectivity towards Cr(VI) compared to Ni(II), and Cu(II) ions.

Adsorption mechanism study

To better understand the adsorption process the XPS spectra before and after adsorption were compared. The Cr 2p3/2 core-level spectrum at about 577.51 eV[45] after Cr(VI) adsorption can be fitted into two peaks with BEs of about 577.68 and 580.58 eV attributable to Cr(III) and Cr(VI), respectively (Fig. 12).[46] The results suggest that the PAN/PANI nanofiber mat shows a strong ability to reduce Cr(VI); 86.2 mol% of Cr(VI) ions were reduced to Cr(III) (as shown in Fig. 12a). The Cr 2p3/2 core-level spectrum of PAN/PANI nanofiber mat after regeneration by NaOH is shown in Fig. 12b. It can be seen that the ratio of Cr(III)/Cr(VI) increased after NaOH treatment. In other words, Cr(VI) was more easy to desorb than Cr(III). The N 1s core-level spectra of PAN/PANI nanofibers before and after adsorption of Cr(VI) are shown in Fig. 13. The ratio of benzenoid amine (–NH–) decreased from 58.7 mol% to 49.4 mol% after

Fig. 10 Plot to determine thermodynamic parameters of Cr(VI) adsorption onto PAN/PANI nanofiber mat.

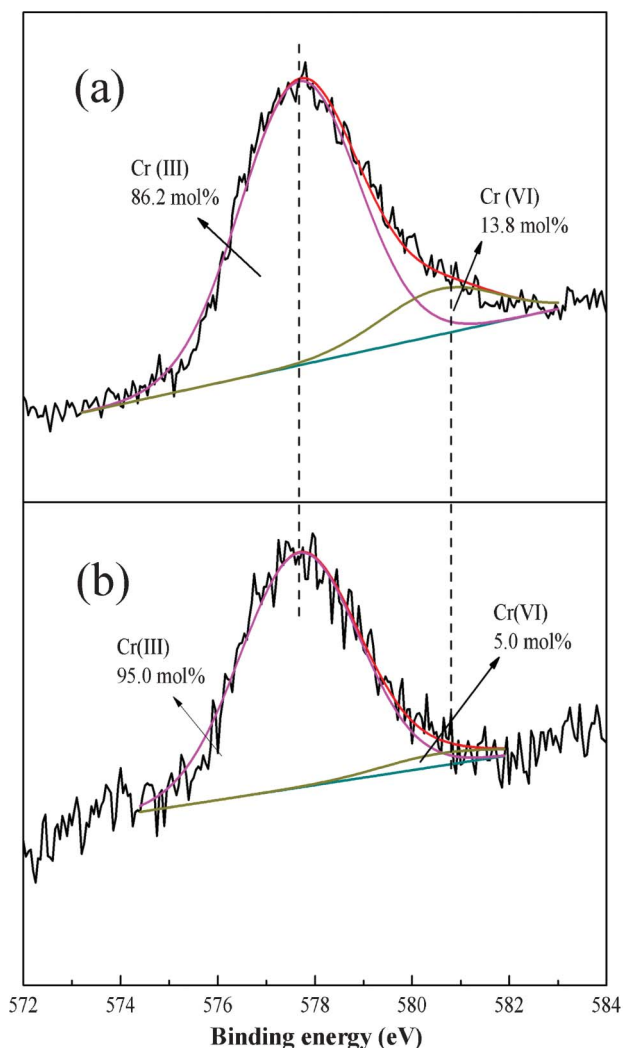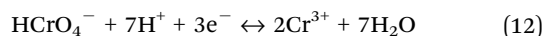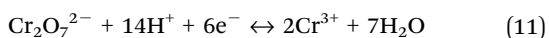Fig. 11 Adsorption performance of PAN/PANI nanofiber mat for a mixed metal ions solution.

Fig. 12 Cr 2p3/2 core level spectra of PAN/PANI nanofiber mat after Cr(VI) adsorption (a), and regeneration (b).

Fig. 13 N 1s core level spectra of PAN/PANI nanofiber mat before (a) and after (b) Cr(VI) adsorption.

adsorption of Cr(VI). However, the ratio of quinoid imine (–N=) increased from 14.9 mol% to 23.9 mol%. Nearly 9 mol% of benzenoid amine was converted to quinoid imine during the adsorption process.

Although one proton and electron will be released during the conversion from benzenoid amine to quinoid imine, protons and electrons can also be used during the reduction process (see eqn (11) and (12)).

$$Cr_2O_7^{2-} + 14H^+ + 6e^- \leftrightarrow 2Cr^{3+} + 7H_2O \qquad (11)$$

$$HCrO_4^- + 7H^+ + 3e^- \leftrightarrow 2Cr^{3+} + 7H_2O \qquad (12)$$

Moreover, more protons are involved in the reduction process than electrons. Therefore, additional protons are needed, and they can be only obtained from the solution leading to a decrease in the solution pH after adsorption of Cr(VI) as shown experimentally in Fig. 14. All the above are
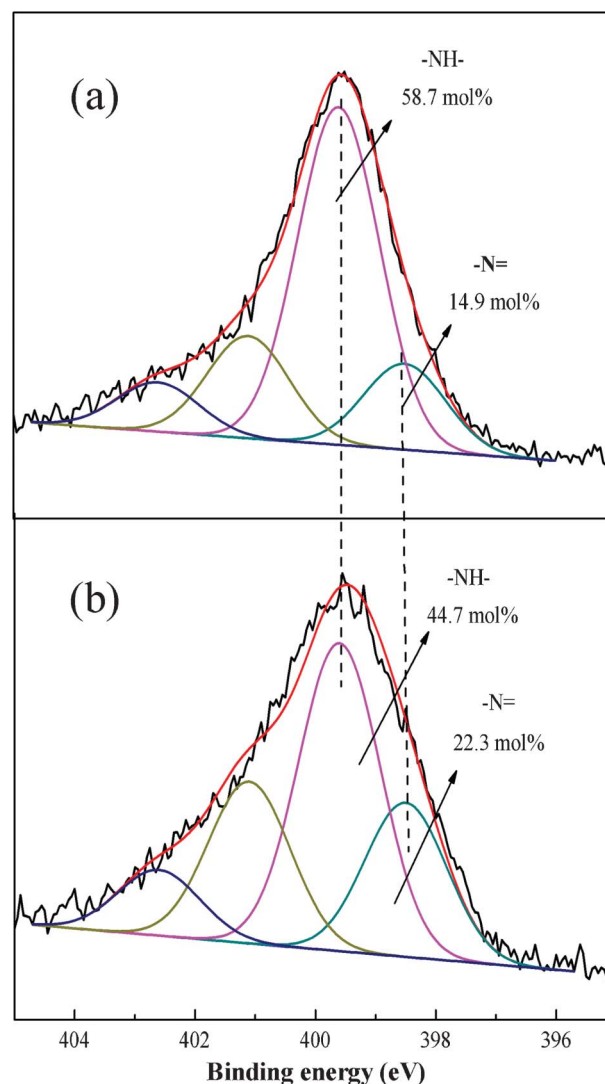
consistent with a redox process with the reduction of Cr(VI) due to the conversion of benzenoid amine to quinoid imine.

Desorption study

Since the adsorption of Cr(VI) ions onto the PAN/PANI nanofiber mat is pH-dependent and a high adsorption capacity was obtained at low pH, the desorption of Cr(VI) ions was carried out by increasing the solution pH. Therefore, for the reusability study, 0.002 M NaOH, 0.01 M NaOH and 0.05 M NaOH were used to regenerate the mats loaded with Cr(VI) ions. As shown in Fig. 15, when the concentration of NaOH was above 0.01 M, the mats showed better reuse performance. The adsorption capacity remains nearly constant after 5 cycles. Interestingly, the adsorption capacity increased after the NaOH treatment. The reason for this increase maybe due to the conversion from emeraldine salt to emeraldine base after treatment with NaOH.[47] In other words, the emeraldine base type polyaniline has higher adsorption capacity than the

Fig. 14 pH change of PAN/PANI nanofiber mat immersed into Cr(VI) solution (a), deionized water (b), and Cr(VI) solution.

emeraldine salt. The decrease of adsorption capacity at low NaOH concentration may be due to the incomplete desorption of Cr ions. In addition, when high concentration of NaOH solution was used, the morphology of PAN/PANI nanofiber mat was affected (Fig. S4, ESI†). The PAN/PANI nanofibers were fused together, and some of the shell materials were broken off from the PAN nanofiber, which might contribute to the increased adsorption capacity. Nevertheless alkali treatment can effectively regenerate the adsorbents.

Conclusions

In summary, we have synthesized PAN/PANI core/shell nanofiber mats by a simple electrospinning method followed by *in situ* polymerization of aniline. The surface morphology of the nanofibers can modified through simple manipulation of

the polymerization temperature. The adsorption performance for Cr(VI) is pH dependent. The adsorption capacity increased with a decrease of solution pH. The adsorption equilibrium was reached within 30 min as the initial solution concentration ranged from 105 to 207 mg L^{-1}, and the sorption capacity increases with temperature. The PAN/PANI nanofiber mat has a strong ability for reduction of Cr(VI), with about 86.2 mol% of Cr(VI) ions reduced to Cr(III). The adsorption follows a pseudo-second-order kinetics model and is best fit using the Langmuir isotherm model. The mats show excellent selectivity towards Cr(VI) ions in the presence of competing ions albeit a small decrease in adsorption is observed. More importantly, the PAN/PANI nanofiber mats can be regenerated and the adsorption properties restored after NaOH treatment.

Notes and references

1 S. A. Katz and H. Salem, *J. Appl. Toxicol.*, 1993, **13**, 217.
2 Y. Liu, D. Yuan, J. Yan, Q. Li and T. Ouyang, *J. Hazard. Mater.*, 2011, **186**, 473.
3 T. Ölmez, *J. Hazard. Mater.*, 2009, **162**, 1371.
4 B. Galán, D. Castañeda and I. Ortiz, *Water Res.*, 2005, **39**, 4317.
5 L. Xing and D. Beauchemin, *J. Anal. At. Spectrom.*, 2011, **26**, 2006.
6 Y. Xing, X. Chen and D. Wang, *Environ. Sci. Technol.*, 2007, **41**, 1439.
7 S. Edebali and E. Pehlivan, *Chem. Eng. J.*, 2010, **161**, 161.
8 S. Gomes, S. A. Cavaco, M. J. Quina and L. M. Gando-Ferreira, *Desalination*, 2010, **254**, 80.
9 I. Korus and K. Loska, *Desalination*, 2009, **247**, 390.
10 A. Hafez and S. El-Manharawy, *Desalination*, 2004, **165**, 141.
11 H.-D. Choi, W.-S. Jung, J.-M. Cho, B.-G. Ryu, J.-S. Yang and K. Baek, *J. Hazard. Mater.*, 2009, **166**, 642.
12 Z. Wu and D. Zhao, *Chem. Commun.*, 2011, **47**, 3332.
13 S. K. Prabhakaran, K. Vijayaraghavan and R. Balasubramanian, *Ind. Eng. Chem. Res.*, 2009, **48**, 2113.
14 Z. Ai, Y. Cheng, L. Zhang and J. Qiu, *Environ. Sci. Technol.*, 2008, **42**, 6955.
15 B. Liu and Y. Huang, *J. Mater. Chem.*, 2011, **21**, 17413.
16 S. He, Y. Zhao, M. Wei and X. Duan, *Ind. Eng. Chem. Res.*, 2011, **50**, 2800.
17 S. He, Y. Zhao, M. Wei, D. G. Evans and X. Duan, *Ind. Eng. Chem. Res.*, 2012, **51**, 285.
18 H. Wang, N. Yan, Y. Li, X. Zhou, J. Chen, B. Yu, M. Gong and Q. Chen, *J. Mater. Chem.*, 2012, **22**, 9230.
19 C.-Y. Cao, P. Li, J. Qu, Z.-F. Dou, W.-S. Yan, J.-F. Zhu, Z.-Y. Wu and W.-G. Song, *J. Mater. Chem.*, 2012, **22**, 19898.
20 Y. Ni, J. Li, L. Jin, J. Xia, J. Hong and K. Liao, *New J. Chem.*, 2009, **33**, 2055.

Fig. 15 Adsorption–desorption cycles.

21 S. Deng, R. Bai and J. P. Chen, *Langmuir*, 2003, **19**, 5058.
22 D. H. Shin, Y. G. Ko, U. S. Choi and W. N. Kim, *Ind. Eng. Chem. Res.*, 2004, **43**, 2060.
23 S. Haider and S.-Y. Park, *J. Membr. Sci.*, 2009, **328**, 90.
24 P. Kampalanonwat and P. Supaphol, *ACS Appl. Mater. Interfaces*, 2010, **2**, 3619.
25 P. K. Neghlani, M. Rafizadeh and F. A. Taromi, *J. Hazard. Mater.*, 2011, **186**, 182.
26 P. Kampalanonwat and P. Supaphol, *Ind. Eng. Chem. Res.*, 2011, **50**, 11912.
27 X. Wang, M. Min, Z. Liu, Y. Yang, Z. Zhou, M. Zhu, Y. Chen and B. S. Hsiao, *J. Membr. Sci.*, 2011, **379**, 191.
28 M. Min, L. Shen, G. Hong, M. Zhu, Y. Zhang, X. Wang, Y. Chen and B. S. Hsiao, *Chem. Eng. J.*, 2012, **197**, 88.
29 Y. Lin, W. Cai, X. Tian, X. Liu, G. Wang and C. Liang, *J. Mater. Chem.*, 2011, **21**, 991.
30 Y. Lin, W. Cai, H. He, X. Wang and G. Wang, *RSC Adv.*, 2012, **2**, 1769.
31 S. Xing, D. Zhao, W. Yang, Z. Ma, Y. Wu, Y. Gao, W. Chen and J. Han, *J. Mater. Chem. A*, 2013, **1**, 1694.
32 T. Yao, T. Cui, J. Wu, Q. Chen, S. Lu and K. Sun, *Polym. Chem.*, 2011, **2**, 2893.
33 M. Bhaumik, A. Maity, V. V. Srinivasu and M. S. Onyango, *J. Hazard. Mater.*, 2011, **190**, 381.
34 Y. Wang, B. Zou, T. Gao, X. Wu, S. Lou and S. Zhou, *J. Mater. Chem.*, 2012, **22**, 9034.
35 J. Wang, K. Pan, Q. He and B. Cao, *J. Hazard. Mater.*, 2013, **244–245**, 121.
36 R. Zhang, H. Ma and B. Wang, *Ind. Eng. Chem. Res.*, 2010, **49**, 10004.
37 X. Gou, G. Fei, H. Su and L. Zhang, *J. Phys. Chem. C*, 2011, **115**, 1608.
38 Y. Zheng, W. Wang, D. Huang and A. Wang, *Chem. Eng. J.*, 2012, **191**, 154.
39 L. Shao, J.-W. Jeon and J. L. Lutkenhaus, *Chem. Mater.*, 2012, **24**, 181.
40 S. Golczak, A. Kanciurzewska, M. Fahlman, K. Langer and J. J. Langer, *Solid State Ionics*, 2008, **179**, 2234.
41 J. Hu, G. Chen and I. M. C. Lo, *Water Res.*, 2005, **39**, 4528.
42 L. Ai, H. Yue and J. Jiang, *Nanoscale*, 2012, **4**, 5401.
43 L. Zhang, H. Wang, W. Yu, Z. Su, L. Chai, J. Li and Y. Shi, *J. Mater. Chem.*, 2012, **22**, 18244.
44 J. Zhou, Y. Cheng, J. Yu and G. Liu, *J. Mater. Chem.*, 2011, **21**, 19353.
45 J. Hu, G. Chen and I. M. C. Lo, *Water Res.*, 2005, **39**, 4528.
46 G. Cappelletti, C. L. Bianchi and S. Ardizzone, *Appl. Catal., B*, 2008, **78**, 193.
47 M. S. Izumi, D. C. Ferreira, R. L. Constantino and L. A. Temperini, *Macromolecules*, 2007, **40**, 3204.